

Conformal dynamics in gauge theories via non-perturbative renormalization group

Haruhiko Terao* and Akito Tsuchiya†

Institute for Theoretical Physics, Kanazawa University, Kanazawa 920-1192, Japan

(Dated: December 17, 2018)

Abstract

The dynamics at the IR fixed point realized in the $SU(N_c)$ gauge theories with massless Dirac fermions is studied by means of the non-perturbative renormalization group. The analysis includes the IR fixed points with non-trivial Yukawa couplings. The renormalization properties of the scalar field are also discussed and it is shown that hierarchical mass scale may be allowed without intense fine-tuning due to a large anomalous dimension.

PACS numbers: 11.10.Hi, 11.25.Hf, 11.30.Rd, 12.38.Lg

arXiv:0704.3659v2 [hep-ph] 19 Oct 2007

*Electronic address: terao@hep.s.kanazawa-u.ac.jp

†Electronic address: tsucchi-@hep.s.kanazawa-u.ac.jp

I. INTRODUCTION

The hierarchy between the Electro-Weak (EW) scale and the fundamental scales, Planck scale or the grand unification scale, has been a long-standing problem in particle physics. Contrary to this, smallness of the QCD scale may be understood as a consequence of the classical scale invariance of QCD, although the scale invariance is broken quantum mechanically. The QCD scale is determined by the so-called dimensional transmutation. However the fundamental scalar theory necessarily allows a relevant operator, the scalar mass term, which causes the gauge hierarchy problem. Indeed the mass term can be forbidden by some symmetries such as supersymmetry. Meanwhile, the relevant operators may be also suppressed, if the dynamics respects the conformal invariance. Therefore, it would be worthwhile to think about the conformal field theories as another possibility to shed light on the hierarchy problem.

Recently, conformal field theories (CFTs) in four dimensions have been also attracting much attention in the context of the so-called AdS/CFT correspondence [1, 2]. Especially, some phenomenological models given in the five dimensional warped space have been studied intensively as new scenarios for the EW symmetry breaking. The typical ones are the Higgsless models, the minimal composite Higgs models and so on [3].

It would be very interesting to find the four-dimensional descriptions of the models given in the five dimensional AdS space. However the AdS/CFT correspondence is rather speculative. Usually explicit CFTs equivalent to the five dimensional models are unknown, although some models are thought to correspond with the walking Technicolor (TC) models [4].

On the other hand, the explicit examples of the non-trivial CFTs are very limited in four dimensions, specially in the non-supersymmetric cases. Indeed it has been well-known for some time that the non-abelian gauge theory becomes a CFT for the appropriate number of flavors. The gauge coupling approaches the so-called Banks-Zaks (BZ) fixed point [5] towards infrared (IR) direction. However, this class of gauge theories would be the unique known example of the CFTs.

In the Ref. [5], the existence of the fixed point was discussed by the zero points of the gauge beta function evaluated perturbatively. Therefore the analysis of the fixed point is reliable only in the weak coupling region. However, the gauge coupling of the BZ fixed point increases rapidly as the number of flavors decreases. Therefore the flavor numbers are found

to be rather limited so as to realize the BZ fixed points in the weak coupling region. Then some non-perturbative analysis is required to clarify the phase diagram for various numbers of flavors.

In this paper we examine the BZ fixed point and the dynamical properties of the CFT even in the strong coupling region by means of the non-perturbative renormalization group (NPRG). So far the phase diagrams of the $SU(N_c)$ gauge theories with various numbers of vector-like fermions have been investigated by solving the Dyson-Schwinger (DS) equations [6, 7, 8]. In these analyses, the two-loop gauge beta function was applied in the approximation scheme. Then it was shown the flavor number N_f should be larger than $4N_c$ in the large N_c leading in order to have the unbroken phase of chiral symmetry. The BZ fixed point should exist in this unbroken phase, since the theory on the fixed point is scale invariant. Thus the conformal window of QCD like theories is given by $16 \geq N_f \geq 12$, while numerical simulation of $SU(3)$ lattice gauge theories indicates the window of $16 \geq N_f \geq 7$ [9].

In the DS approach, the ladder approximation is frequently applied due to its simplicity. It has been known that the exactly same results of the chiral phase boundary and the order parameter can be obtained by solving the NPRG equations [10, 11]. Moreover, the DS equations are given with respect to the order parameter and, therefore, we can study only the symmetry broken phase. Contrary to this, the NPRG enable us to describe the RG flows and the fixed points irrespective of the phases. Therefore, the RG approach is very suitable to study of the conformal dynamics around the fixed point as well as the phase structures [11]. In addition, it will be found that the approximation can be improved easily beyond the so-called ladder approximation in a somewhat systematic way in the NPRG. We will perform the RG analysis with an improved framework from the conventional one later. The phase structure of QCD with many flavors has been also studied by the NPRG method [12].

Thanks to the simplicity of the NPRG equations, we may easily extend the analysis to gauge-Yukawa models with introducing a gauge singlet scalar field. Then it is found that the BZ fixed point becomes unstable and an IR fixed point with a non-trivial Yukawa coupling appears as a stable fixed point instead. We will show the conformal dynamics around the new fixed point and the phase diagram obtained by the NPRG analysis.

As is well known, the mass parameter of a scalar field is relevant and fine-tuning is required in order to adjust it near the critical surface, or to make a large hierarchy in the mass scales. However the scalar field acquires a large anomalous dimension at the IR fixed

point, if the fixed point interaction is strong. Then the anomalous dimension suppresses the mass parameter towards the IR direction and the power of renormalization scale dependence may be reduced to even almost logarithmic. Therefore the fine-tuning aspect turns out to be very different from that given in the weak coupling region.

Recently, Luty and Okui [13] considered a composite Higgs model, where the strong dynamics is approximately conformal and the Higgs field is endowed with a large anomalous dimension. This model is given in the chiral symmetry broken phase of a QCD like gauge theory and, however, is near the ultra-violet (UV) fixed point, which will be discussed later. One of the author also proposed another type of the Higgs model [14], which makes use of the IR fixed point with a non-trivial Yukawa coupling. There the fine-tuning problem of the standard model (SM) Higgs may be ameliorated owing to the large anomalous dimension. Thus knowledge of the conformal dynamics of gauge theories seems to be very useful even in phenomenological studies, specially, of the Higgs sector.

This paper is organized as follows. We start in section II with perturbative analysis of the IR fixed point for the gauge-Yukawa models. In section III, we develop the NPRG equations for the $SU(N_c)$ gauge theory with N_f massless flavors. Section IV addresses the fixed points, anomalous dimensions as well as the phase diagrams of the gauge theories by solving the NPRG equations. In section V, we extend the RG analysis to the gauge-Yukawa model and study the conformal dynamics around the IR fixed point with a non-trivial Yukawa coupling. The effect of the large anomalous dimension of the scalar field is also examined in section VI. Finally section VII is devoted to the conclusions and discussions.

II. PERTURBATIVE ANALYSIS OF THE IR FIXED POINTS

A. Banks-Zaks (BZ) fixed point

It is well-known that a IR fixed point, called the BZ fixed point [5], realizes in an asymptotically free gauge theory with appropriate numbers of flavors. When we add a gauge singlet scalar field coupled through Yukawa interaction with the fermions, then the BZ fixed point becomes unstable. In some cases, the RG flows are found to approach a new fixed point with non-vanishing Yukawa coupling. In this section, let us discuss the fixed points by using the perturbative RG equations.

We restrict our discussion to the $SU(N_c)$ gauge theories with N_f massless flavors of the N_c dimensional representation. The two loop beta function for the gauge coupling $\alpha_g = g^2/(4\pi)^2$ is found to be

$$\mu \frac{d\alpha_g}{d\mu} = -2b_0\alpha_g^2 - 2b_1\alpha_g^3 + \dots, \quad (1)$$

where the coefficients are given with the quadratic Casimir $C_2(N_c) = (N_c^2 - 1)/2N_c$ as

$$b_0 = \frac{11}{3}N_c - \frac{2}{3}N_f, \quad (2)$$

$$b_1 = \frac{34}{3}N_c^2 - \frac{N_f}{2} \left(4C_2(N_c) + \frac{20}{3}N_c \right). \quad (3)$$

The IR fixed point exists when $b_0 > 0$ and $b_1 < 0$. This constrains the conformal window for N_f to be $(34/13)N_c < N_f < (11/2)N_c$ in the large N_c leading. The value of the fixed point gauge coupling, $\alpha_g^* = -b_0/b_1$, increases as N_f decreases. As long as this fixed point coupling is sufficiently small, or N_f is close to $(11/2)N_c$, the perturbative analysis is reliable.

However the lower bound of the conformal window is not meaningful in practice, since the fixed point gauge coupling is very strong with the flavor number near the lower bound. Then such perturbative calculation is not reliable. Indeed, the three-loop beta function reduces the gauge coupling at the fixed point considerably. It does not mean that the three-loop result is more reliable though, since the beta functions calculated by perturbation give an asymptotic series. Although it would be better to use the beta function evaluated *e.g.* by means of the Borel summation instead, it is beyond our present scope. In this paper, we use the two-loop beta function simply as the primitive step of the analysis. Moreover, it is found that such strong gauge interaction induces spontaneous chiral symmetry breaking and erases the fixed point. It will be shown that the NPRG analysis combined with the two-loop gauge beta function leads to the conformal window given by $4N_c < N_f < (11/2)N_c$, which coincides with the result obtained by analyzing the ladder DS equations [6].

In the following discussions, the anomalous dimension of the fermion mass operator $\bar{\psi}\psi$ plays an important role. The anomalous dimension $\gamma_{\bar{\psi}\psi}$ evaluated at the one-loop level is $-6C_2(N_c)\alpha_g$. We note that this anomalous dimension is negative at the BZ fixed point. This implies that the Yukawa coupling with a gauge singlet scalar is relevant there, since the dimension of the operator $\phi(\bar{\psi}\psi)$ is less than 4. Thus it is seen that the BZ fixed point become unstable under perturbation by the Yukawa interactions.

B. Yukawa interaction with a “meson” field

First let us consider to incorporate a Yukawa interaction respecting the flavor symmetry of the unperturbed theory. The flavor symmetry of the gauge theory with N_f massless flavors is $U(N_f)_L \times U(N_f)_R$, although the axial $U(1)$ part is broken by anomaly. We introduce a “meson”-like scalar Φ , which transforms as $\Phi \rightarrow g_L \Phi g_R^\dagger$ with the group elements $g_{L(R)}$ of $U(N_f)_{L(R)}$. The invariant Yukawa interaction is given by

$$\mathcal{L} \sim -y \Phi_j^i \bar{\psi}_{Li} \psi_R^j + \text{h.c.} \quad (4)$$

Then the beta functions for the gauge coupling $\alpha_g = g^2/(4\pi)^2$ and the Yukawa coupling $\alpha_y = |y|^2/(4\pi)^2$ are found to be [15]

$$\mu \frac{d\alpha_g}{d\mu} = -2b_0\alpha_g^2 - 2b_1\alpha_g^3 - 2N_f^2\alpha_g^2\alpha_y, \quad (5)$$

$$\mu \frac{d\alpha_y}{d\mu} = 2\alpha_y [(2N_c + N_f)\alpha_g - 6C_2(N_c)\alpha_g]. \quad (6)$$

Here we evaluate the Yukawa beta function at the one-loop order.

It is found from these beta functions that the IR fixed point exists only for $5.24 < N_f/N_c < 5.5$ in the large N_c leading and the fixed point gauge couplings are very small in any case [26]. When the flavor number is less than this window, then the RG flow goes infinity eventually. This is because the non-trivial zero point of the two-loop gauge beta function is eliminated by a small Yukawa coupling. The one-loop approximation of the Yukawa beta coupling is not the origin. Therefore if we use the three-loop beta function or some non-perturbative beta function for the gauge coupling, then the result may different. This is beyond our present scope and we do not consider this type of gauge-Yukawa models.

C. Yukawa interaction with a singlet scalar

Next we consider the Yukawa coupling with a flavor singlet scalar ϕ such as

$$\mathcal{L} \sim -\phi \sum_{i=1}^{n_f} y_i \bar{\psi}_{Li} \psi_R^i + \text{h.c.}, \quad (7)$$

where $n_f = 1, \dots, N_f$. The Yukawa couplings can be diagonal zed by the flavor rotation. We note that these Yukawa couplings break the flavor symmetry of $U(N_f)_L \times U(N_f)_R$ explicitly.

The RG equations for the gauge coupling and the Yukawa coupling are given explicitly by [15]

$$\mu \frac{d\alpha_g}{d\mu} = -2b_0\alpha_g^2 - 2b_1\alpha_g^3 - 2\alpha_g^2 \sum_{i=1}^{n_f} \alpha_{y_i}, \quad (8)$$

$$\mu \frac{d\alpha_{y_i}}{d\mu} = 2\alpha_{y_i} \left[2N_c \sum_{j=1}^{n_f} \alpha_{y_j} + \alpha_{y_i} - 6C_2(N_c)\alpha_g \right], \quad (9)$$

where we used the one-loop beta function for the Yukawa coupling again. Extension of the Yukawa beta function to the two-loop [15] order does not alter the fixed point structure significantly, although 2-loop terms are essential for the gauge beta function to see the BZ fixed point.

Let us examine the fixed point with non-trivial Yukawa couplings. We may set $y_i = y^*$, since the Yukawa couplings are expected to be the same at the IR fixed point. Then the explicit beta functions, (1) and (9), lead the non-trivial fixed point couplings α_g^* and α_y^* given by

$$\alpha_g^* = \frac{b_0}{-b_1 + \frac{6C_2(N_c)n_f}{2N_cn_f+1}} \simeq \frac{b_0}{-b_1 + 3/2}, \quad (10)$$

$$\alpha_y^* = \frac{6C_2(N_c)}{2N_cn_f+1} \alpha_g^* \simeq \frac{3}{2n_f} \alpha_g^*, \quad (11)$$

in the large N_c leading. Thus the new IR fixed point is found to always appear, since $b_1 < 0$ for existence of the BZ fixed point. We will examine the dynamics in this type of gauge-Yukawa models by means of the NPRG in section V and section VI.

III. NON-PERTURBATIVE RG FOR GAUGE THEORIES

A. Approximation scheme and NPRG equations

In practice it is a quite difficult problem to extend the RG equations to ones fully reliable even in the non-perturbative region. Here we consider to apply the so-called exact renormalization group (ERG) [19] reduced by some approximation scheme, which we call the NPRG. It has been found [10, 11] that the NPRG method can also describe the spontaneous chiral symmetry breaking phenomena induced by strong gauge interaction and reproduces the results obtained by solving the DS equations. We first review the formulation briefly.

The ERG equation gives evolution of the Wilsonian effective action under infinitesimal shift of the cutoff scale. Although it is amusing that the evolution can be represented exactly as a functional equation with respect to the Wilsonian effective action, it is necessary to reduce the equations by some approximation in order to analyze them. It is usually performed to truncate the series of local operators in the Wilsonian effective action. Improvement of the approximation is made by increasing the level of the operator truncation.

Once the operator truncation is performed, then the ERG equation turns out to be a set of one-loop RG equations. Difference from the perturbative RG lies in the point that couplings of the higher dimensional operators are involved as well as the renormalizable operators. This procedure enables us to sum up an infinite number of loop diagrams.

It was found through the previous studies [10] that the effective four-Fermi operators are found to play an important role for the non-perturbative analysis of the chiral symmetry breaking. The reason may be understood by thinking over the anomalous dimension of the fermion mass operator $\gamma_{\bar{\psi}\psi}$. Fig. 1 shows schematically how the anomalous dimension is represented in terms of the effective four-Fermi couplings in the NPRG framework. The four-Fermi couplings are also given as a sum of infinitely many loop diagrams by solving the RG equations. Thus a non-perturbative sum of the loop diagrams is carried out by incorporating the four-Fermi operators.

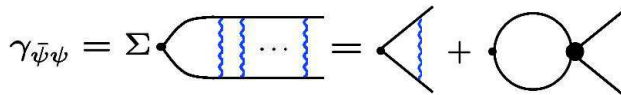


FIG. 1: The anomalous dimension $\gamma_{\bar{\psi}\psi}$ in terms of the effective four-Fermi γ vertex is shown schematically.

Here we shall consider the four-Fermi operators induced in the Wilsonian effective action of the gauge theory. The four-Fermi operators should be invariant under the color $SU(N_c)$ as well as the flavor symmetry $U(N_f)_L \times U(N_f)_R$. Among many invariant operators, we take only the following operators [27],

$$\mathcal{O}_S = 2\bar{\psi}_{Li}\psi_R^j \bar{\psi}_{Rj}\psi_L^i, \quad (12)$$

$$\mathcal{O}_V = \bar{\psi}_{Li}\gamma_\mu\psi_L^j \bar{\psi}_{Lj}\gamma_\mu\psi_L^i + (L \leftrightarrow R), \quad (13)$$

$$\mathcal{O}_{V1} = 2\bar{\psi}_{Li}\gamma_\mu\psi_L^i \bar{\psi}_{Rj}\gamma_\mu\psi_R^j, \quad (14)$$

$$\mathcal{O}_{V2} = (\bar{\psi}_{Li}\gamma_\mu\psi_L^i)^2 + (L \leftrightarrow R). \quad (15)$$

Then the four-fermi part of the Wilsonian effective Lagrangian is given by

$$-\mathcal{L}_{\text{eff}} \sim \frac{G_S(\Lambda)}{\Lambda^2} \mathcal{O}_S + \frac{G_V(\Lambda)}{\Lambda^2} \mathcal{O}_V + \frac{G_{V1}(\Lambda)}{\Lambda^2} \mathcal{O}_{V1} + \frac{G_{V2}(\Lambda)}{\Lambda^2} \mathcal{O}_{V2}, \quad (16)$$

where the couplings G are dimensionless. The operators which contain the $SU(N_c)$ generators T^A may be reduced to the above operators by performing the Fierz transformation; *e.g.*

$$\sum_A \bar{\psi}_{Li} T^A \gamma_\mu \psi_L^i \bar{\psi}_{Rj} T^A \gamma_\mu \psi_R^j = -\frac{C_2(N_c)}{N_c} \mathcal{O}_S + \dots, \quad (17)$$

$$\sum_A \left[(\bar{\psi}_{Li} T^A \gamma_\mu \psi_L^i)^2 + (L \leftrightarrow R) \right] = \frac{C_2(N_c)}{N_c} \mathcal{O}_V + \dots. \quad (18)$$

We also discard the higher dimensional operators containing covariant derivatives in the lowest order of truncation. It is noted that the four-fermi operators are not induced through any local operators with 8 fermions or more. Therefore the RG flows of the four fermi couplings are not influenced by the higher dimensional operators as long as we take only the local operators.

We should also incorporate higher dimensional operators of the field strength, such as $(D_\mu F^{\mu\nu})^2$, $(F_{\mu\nu} F^{\mu\nu})^2$ and so on. Otherwise the higher loop part of the gauge beta function in Eq. (1) is not reproduced. However practical calculations of the loop diagrams are rather tedious. It is also a hard problem to maintain the gauge invariance in the Wilson RG, since the RG is defined with cutoff the momentum scale. For the recent approach to this problem, see Refs. [20]. In addition, it would be enough to follow the RG flow of the gauge coupling only for the present purpose. Therefore we do not deal with the ERG equations faithfully, but substitute the two-loop beta function (1) for the RG equation of the gauge coupling instead. The approximation scheme of the present analysis is given by these procedures.

B. The RG equations

Now it is enough to deduce the RG equations for the four-fermi couplings G_S , G_V , G_{V1} and G_{V2} in the simplified scheme explained above. Calculation of the RG equations is rather lengthy but straightforward. In Appendix, we consider the one-loop corrections by the gauge interaction explicitly and illustrate how we may calculate the RG equations with these examples. Then it is found that only the four-fermi couplings G_S and G_V are induced.

It is also shown that the gauge corrections are dependent on the gauge choice. Here we take the Landau gauge, in which the wave function renormalization of the fermions vanishes.

There are also other loop diagrams incorporating two four-fermi operators and so on. The resultant RG equations are shown in Appendix. In the followings analysis, however, we extract the large N_c and N_f leading part from them for the simplicity. Then it is seen that the equations for G_S and G_V decouple from G_{V1} and G_{V2} . Besides the couplings G_{V1} and G_{V2} are not induced at all, if their initial values are vanishing. Thus it is all right to examine the RG equations for G_S and G_V , which are given explicitly by

$$\Lambda \frac{dg_S}{d\Lambda} = 2g_S - 2N_c \left(g_S + \frac{3}{2}\alpha_g \right)^2 + 2N_f g_S g_V, \quad (19)$$

$$\Lambda \frac{dg_V}{d\Lambda} = 2g_V + (N_c + N_f)g_V^2 + \frac{1}{4}N_f g_S^2 - \frac{3}{4}N_c \alpha_g^2, \quad (20)$$

where we rescaled the couplings as $g_{S(V)} = G_{S(V)}/(4\pi^2)$. We solve the RG equations (19) and (20) coupled with the two-loop gauge beta function in the large N_c and N_f leading,

$$\Lambda \frac{d\alpha_g}{d\Lambda} = -2N_c \left(\frac{11}{3} - \frac{2N_f}{3N_c} \right) \alpha_g^2 - 2N_c^2 \left(\frac{34}{3} - \frac{13N_f}{3N_c} \right) \alpha_g^3. \quad (21)$$

On the other hand, solutions of the DS equations are usually given by sum of the ladder diagrams as shown in Fig. 1. Therefore most of the analyses using the SD equations have been carried out in the ladder approximation. We may restrict the loop corrections taken in the RG equations (19) and (20) to the ladder diagrams as well. Then the last term in Eq. (19) is found to drop out and the RG equation is reduced to

$$\Lambda \frac{dg_S}{d\Lambda} = 2g_S - 2N_c \left(g_S + \frac{3}{2}\alpha_g \right)^2. \quad (22)$$

It is noted that the coupling g_V is not involved with evolution of g_S any more. However the flavor number N_f must be fairly large in the cases involving the BZ fixed point. Therefore the last term in Eq. (19) is supposed to give a sizeable effect. In the next section, we also solve Eq. (22) in order to compare the results with those obtained in the ladder approximation.

IV. FIXED POINTS AND ANOMALOUS DIMENSIONS

The two-loop gauge beta function (1) gives the fixed point coupling as

$$N_c \alpha_g^* = \frac{11 - 2r}{13r - 34}, \quad (23)$$

where $34/13 < r = N_f/N_c < 11/2$. However, this condition for the flavor number does not always guarantee existence of the IR fixed point. All the other couplings must approach their fixed point values. The fixed point for the four-fermi coupling g_S in the ladder approximation can be found analytically from the RG equation (22). Those are given by

$$N_c g_S^* = \frac{1}{2} \left(1 - 3N_c \alpha_g^* \pm \sqrt{1 - 6N_c \alpha_g^*} \right), \quad (24)$$

where the solution with $+(-)$ gives the UV(IR) fixed point.

It is noted that the fixed point does not exist for $N_c \alpha_g^* > 1/6$ and the four-fermi coupling g_S of any RG flow goes to infinity. This behavior of the RG flows shows that there is only broken phase of the chiral symmetry [10]. Then the conformal window is found to be

$$4N_c \leq N_f \leq \frac{11}{2}N_c, \quad (25)$$

in the large N_c leading. However we should keep in mind that the lower bound of this window is not robust owing to large dependence on the gauge beta function, as was mentioned in section II.

It is easy to find the fixed points in the non-ladder approximation numerically from Eqs. (19) and (20). Then the fixed point couplings are given by $(\alpha_g^*, g_S^*, g_V^*)$. In Fig. 2, the couplings $N_c(\alpha_g^*, g_S^*)$ of the IR (BZ) fixed points and the UV fixed points are shown by taking $r = N_f/N_c$ to be a continuous parameter. For the comparison, the fixed points obtained from Eq. (24) in the ladder approximation are also shown by dotted line.

We may figure out the RG flows in the coupling space of (α_g, g_S, g_V) by solving the RG equations numerically. Fig. 3 shows some RG flows approaching the BZ fixed point, which is represented by the point A, in the case of $r = N_f/N_c = 4.1$ for an illustration. The points B and C stand for the UV fixed points. It is seen how these fixed points are linked by the renormalized trajectories. The renormalized trajectory connecting the fixed points B and C lies in the phase boundary. Some of the flows go along the critical surface and approach the renormalized trajectory.

In Fig. 4 the RG flows in the cross section of $\alpha_g = \alpha_g^*$ are also shown. The critical surface in the (g_S, g_V) space as well as the renormalized trajectory connecting the fixed points A and B are clearly seen. In the lower phase, where all RG flows approach the IR fixed point, the IR theory appears as a CFT. On the other hand, the chiral symmetry is spontaneously broken in the upper phase, where the four-fermi coupling g_S goes to infinity.

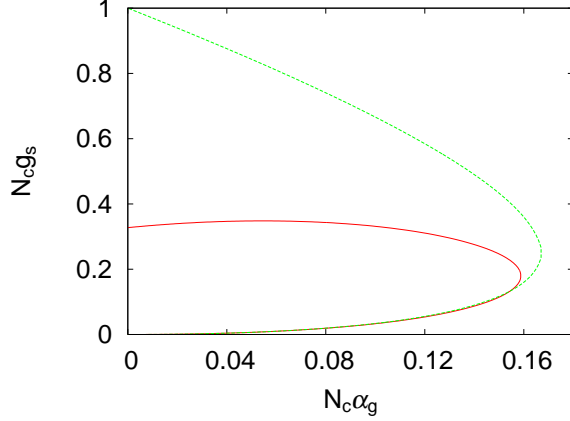


FIG. 2: The couplings $N_c(\alpha_g^*, g_s^*)$ of the IR (BZ) fixed points and the UV fixed points are shown by taking $r = N_f/N_c$ to be a continuous parameter. The dotted line represent the fixed points obtained in the ladder approximation.

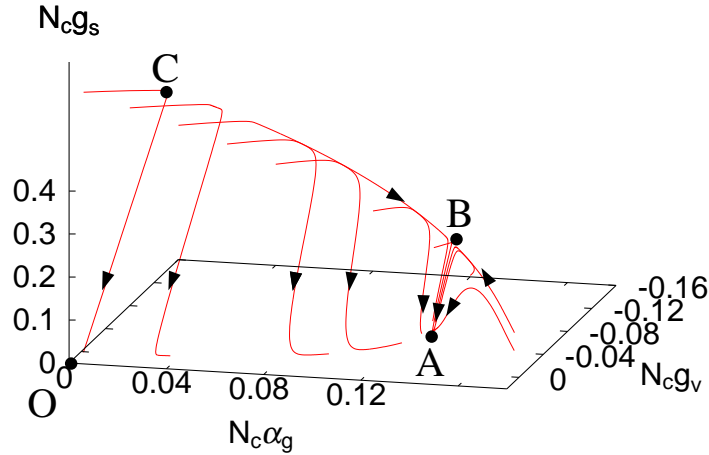


FIG. 3: The fixed points and some RG flows towards the IR direction are shown in the coupling space of $N_c(\alpha_g, g_s, g_v)$ for $r = N_f/N_c = 4.1$ as an example. The point A represents the BZ fixed point. The points B and C stand for UV fixed points and the line connecting them lies in the phase boundary.

The phase divides the cutoff gauge theories given with various gauge couplings into two classes. The critical value of the gauge coupling α_g^{cr} can be read off from the phase diagram. In Fig. 5, $N_c \alpha_g^{\text{cr}}$ is shown for various $r = N_f/N_c$. The dotted line stands for the critical gauge coupling obtained in the ladder approximation.

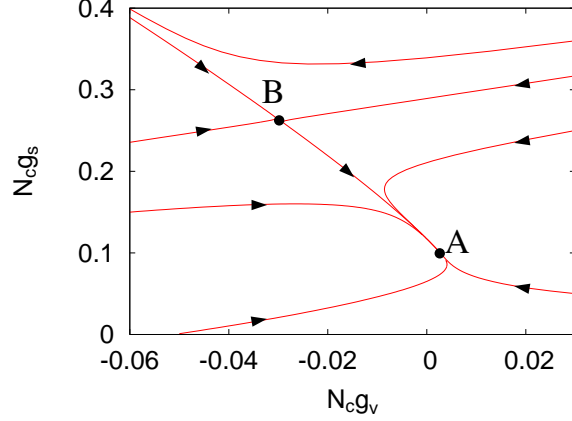


FIG. 4: The RG flows and the fixed points A and B in the cross section of $\alpha_g = \alpha_g^*$ are shown for $r = N_f/N_c = 4.1$.

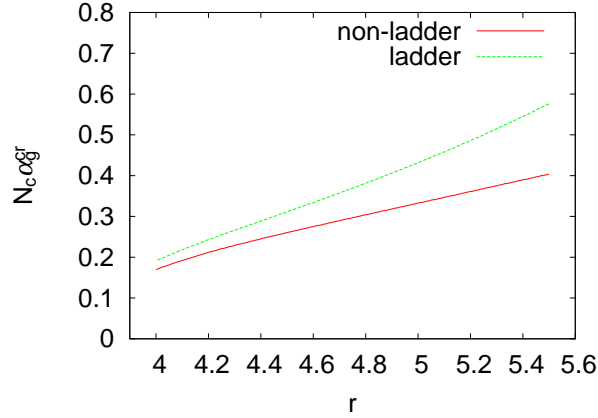


FIG. 5: The critical gauge coupling $N_c \alpha_g^{cr}$ is given for various $r = N_f/N_c$. The dotted line stands for the same obtained in the ladder approximation.

Next we discuss the anomalous dimension of the four-fermi operators at the fixed points A and B. It should be also stressed that the NPRG offers us the right method to evaluate the anomalous dimensions, since they are obtained directly from the RG equations. First we shall consider the anomalous dimensions of the four-fermi operators, which may be easily evaluated by taking infinitesimal deviation of the four-fermi couplings from the fixed point, $g_S = g_S^* + \delta g_S$ and $g_V = g_V^* + \delta g_V$. Then the deviations follow the RG equations,

$$\Lambda \frac{d}{d\Lambda} \begin{pmatrix} \delta g_S \\ \delta g_V \end{pmatrix} = \begin{pmatrix} 2 - 4N_c g_S^* - 6N_c \alpha_g^* + 2N_f g_V^* & 2N_f g_S^* \\ (1/2)N_f g_S^* & 2 + (N_c + N_f)g_V^* \end{pmatrix} \begin{pmatrix} \delta g_S \\ \delta g_V \end{pmatrix}. \quad (26)$$

The eigenvalues of the matrix in the right hand side, which we write by λ_1 and λ_2 ($\lambda_1 < \lambda_2$),

represent nothing but the scaling dimensions of the four-fermi couplings. The four-fermi operators for the eigenmodes, \mathcal{O}_1 and \mathcal{O}_2 , are given by linear combinations of \mathcal{O}_S and \mathcal{O}_V . Then the anomalous dimensions of these operators are given by $\gamma_{\mathcal{O}_i}^* = \lambda_i - 2$ ($i = 1, 2$).

It is found that the both eigenvalues are positive at the IR fixed point A. This means that there is no relevant operators at the fixed point. On the other hand, λ_1 turns out to be negative at the UV fixed point B. This relevant direction gives the renormalized trajectory towards the IR fixed point. In Fig. 6, the anomalous dimensions $|\gamma_{\mathcal{O}_1}^*|$ are shown with respect to the fixed point gauge couplings $N_c\alpha_g^*$.

In the ladder approximation, the anomalous dimension of the four-fermi operator \mathcal{O}_S may be evaluated analytically. It is found from the RG equation (22) immediately as

$$\gamma_{\mathcal{O}_S}^* = -4N_c g_S^* - 6N_c \alpha_g^* = -2 \left(1 \pm \sqrt{1 - 6N_c \alpha_g^*} \right). \quad (27)$$

This should be compared with $\gamma_{\mathcal{O}_1}^*$ evaluated in the non-ladder calculation. The dashed line in Fig. 6 stands for $|\gamma_{\mathcal{O}_S}^*|$ in the ladder approximation. It is seen that the anomalous dimension of the relevant four-fermi operator becomes slightly larger by incorporating the non-ladder diagrams, but the difference is not significant.

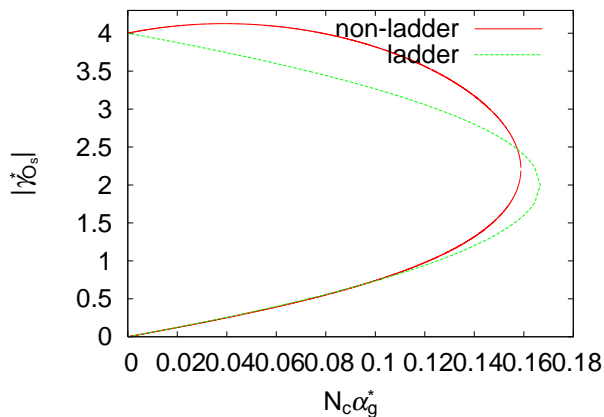


FIG. 6: The anomalous dimensions $|\gamma_{\mathcal{O}_1}^*|$ at the fixed points with respect to α_g^* for various flavor numbers are shown. The dashed line stands for $|\gamma_{\mathcal{O}_S}^*|$ obtained in the ladder approximation.

Another important quantity in our discussion is the anomalous dimension of the fermion mass operator $\bar{\psi}\psi$. It may be evaluated by introducing an infinitesimally small mass to the vector-like fermions. The anomalous dimension is found to be

$$\gamma_{\bar{\psi}\psi} = -6C_2(N_c)\alpha_g - 2N_c g_S + 8g_{V1} \simeq -N_c(3\alpha_g + 2g_S), \quad (28)$$

in the large N_c leading. In the ladder approximation, it is easily obtained as

$$\gamma_{\bar{\psi}\psi}^* = \frac{1}{2}\gamma_{(\bar{\psi}\psi)^2}^* = 1 \pm \sqrt{1 - 6N_c\alpha_g^*}. \quad (29)$$

This result at the UV fixed point has been also found by solving the ladder DS equation [21]. Fig. 7 shows the anomalous dimension $|\gamma_{\bar{\psi}\psi}^*|$ with respect to the fixed point gauge coupling $N_c\alpha_g^*$ for various flavor numbers. The dashed line stands for the same in the ladder approximation. Contrary to the anomalous dimensions of the four-fermi operator, $|\gamma_{\bar{\psi}\psi}^*|$ obtained in the non-ladder approximation are rather different from Eq. (29). However, the anomalous dimensions at the IR fixed point are fairly stable under improvement of the approximation. Therefore, the results may be thought to be reliable even in the strong coupling region. This is a good point of our analysis, since the explicit values of the anomalous dimensions $|\gamma_{\bar{\psi}\psi}^*|$ will be important in the following observations.

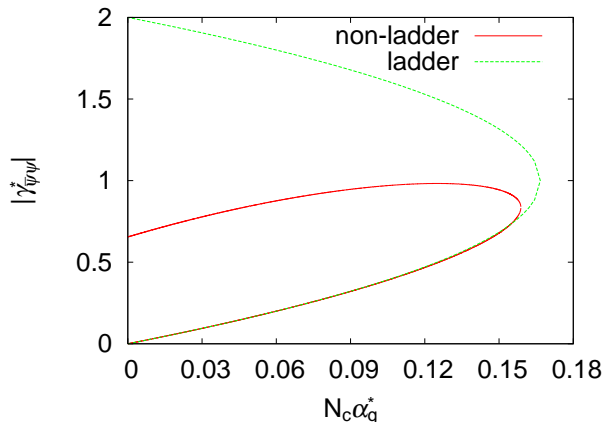


FIG. 7: The anomalous dimensions $|\gamma_{\bar{\psi}\psi}^*|$ at the fixed points. The dashed line stands for the same in the ladder approximation.

V. IR FIXED POINT IN THE GAUGE-YUKAWA MODELS

Now we extend the previous analysis to the gauge-Yukawa models. We consider the Yukawa interaction with a flavor singlet scalar ϕ given by Eq. (7). In order to examine dynamics around the IR fixed point, let us set all Yukawa coupling to be equal, $y_i = y$ ($i = 1, \dots, n_f$).

The flavor symmetry is explicitly broken by the Yukawa interaction. Therefore the operators, which are not invariant under $U(N_f)_L \times U(N_f)_R$, such as $\bar{\psi}_{Li}\psi_R^i$, $\bar{\psi}_{Rj}\psi_L^j$ and

$\bar{\psi}_{Li}\gamma_\mu\psi_L^j$ $\bar{\psi}_{Rj}\gamma_\mu\psi_R^i$ are induced by loop corrections. However the diagrams with scalar lines may be just omitted as sub leading contributions in the large N_c and N_f leading. Therefore we do not have to incorporate other four-fermi operators than \mathcal{O}_S and \mathcal{O}_V in this limit. Besides, we may apply the same beta functions for the four-fermi couplings as well as for the gauge beta function used in the previous section. Only the RG equation of the Yukawa coupling should be modified.

The RG equation of the Yukawa coupling $\alpha_y = |y|^2/(4\pi)^2$ is given in terms of the anomalous dimensions of the scalar field γ_ϕ and $\gamma_{\bar{\psi}\psi}$ as

$$\Lambda \frac{d\alpha_y}{d\Lambda} = 2\alpha_y (\gamma_\phi + \gamma_{\bar{\psi}\psi}). \quad (30)$$

Here it is noted that the four-fermi operators are also involved in the anomalous dimension $\gamma_{\bar{\psi}\psi}$ in the NPRG framework. Explicitly the anomalous dimensions are given by

$$\gamma_\phi = 2N_c n_f \alpha_y, \quad (31)$$

$$\gamma_{\bar{\psi}\psi} = \alpha_y - 6C_2(N_c)\alpha_g - 2N_c g_S + 8g_{V1}. \quad (32)$$

Therefore the beta function for the Yukawa coupling is found to be

$$\Lambda \frac{d\alpha_y}{d\Lambda} \simeq 2\alpha_y [2N_c n_f \alpha_y - 3N_c \alpha_g - 2N_c g_S], \quad (33)$$

in the large N_c leading.

At the IR fixed point, if it exists, the beta function of the Yukawa coupling should vanish. Therefore the anomalous dimension γ_ϕ and the value of the Yukawa coupling α_y^* at the fixed point are simply given by

$$\gamma_\phi^* = 2n_f N_c \alpha_y^* = -\gamma_{\bar{\psi}\psi}^*, \quad (34)$$

which is always positive. In this simple approximation scheme, the beta functions for α_g, g_S, g_V are independent of the Yukawa coupling. Therefore the IR fixed point with a non-trivial Yukawa coupling exists in any case in the conformal window. The anomalous dimension $\gamma_{\bar{\psi}\psi}^*$ as well as the fixed point couplings of $(\alpha_g^*, g_S^*, g_V^*)$ are the same as those given at the BZ fixed point. Therefore the lines shown in Fig. 7 also represent the anomalous dimension of the scalar field γ_ϕ^* at the IR fixed points.

In Fig. 8, the RG flows and the fixed points are described in the coupling space of $N_c(\alpha_y, \alpha_g, g_S)$ in the case of $N_f = 4.1N_c$ and $n_f = 1$. These flows are obtained by solving

the RG equations in the ladder approximation for simplicity. The point A' stands for the IR fixed point of the gauge-Yukawa theory, while the point A represents the BZ fixed point. The fixed points, A, B, B' are all unstable towards the IR direction and are linked by the renormalized trajectories as shown in Fig. 8.

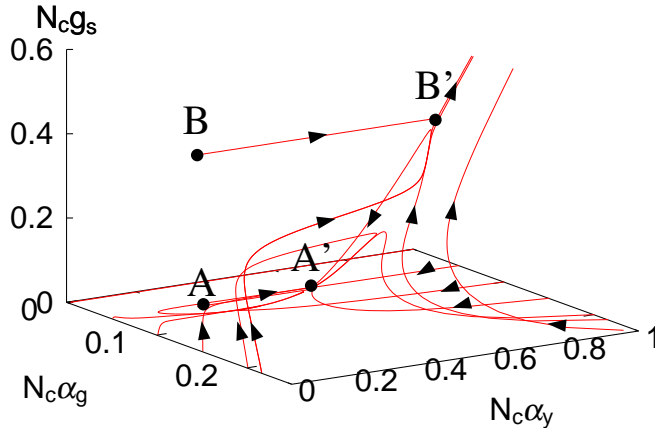


FIG. 8: The RG flows are described in the case of $N_f/N_c = 4.1$ and $n_f = 1$. The blob points A, A', B, B' represent the fixed points. The point A' is the IR fixed point, while A is the BZ fixed point.

Fig. 9 also describes the RG flows in the same case so that the critical surface of the gauge-Yukawa theory is seen clearly. All the flows correspond to theories near critical in the unbroken phase. The phase structure of the gauge-Yukawa theories has been also studied by means of the DS method [22, 23]. In Ref. [22], the RG flows in the broken phase are also given, but with fixed gauge coupling constants. The points C and C' represent the UV fixed point of the pure four-fermi theories and of the four-fermi theories with Yukawa interaction. It is also found how the fixed points are linked with the renormalized trajectories.

When N_f is equal to $4N_c$, then the UV fixed point B' (B) and the IR fixed point A' (A) coincide with each other and the relevant four-fermi operator becomes exactly marginal at the fixed point. In practice, however, the non-leading contributions with respect to N_c and N_f expansion cannot be neglected. Let us also examine an explicit case of $N_c = 3$ and $N_f = 12$ as an example. Then the gauge coupling of the BZ fixed point is given by $\alpha_g^* = 0.06$, which is slightly less than the maximal coupling $\alpha_{g,\max}^* = 1/12C_2(N_c) = 1/16$ in the conformal window [7, 8]. For the gauge-Yukawa theories, we apply the gauge beta

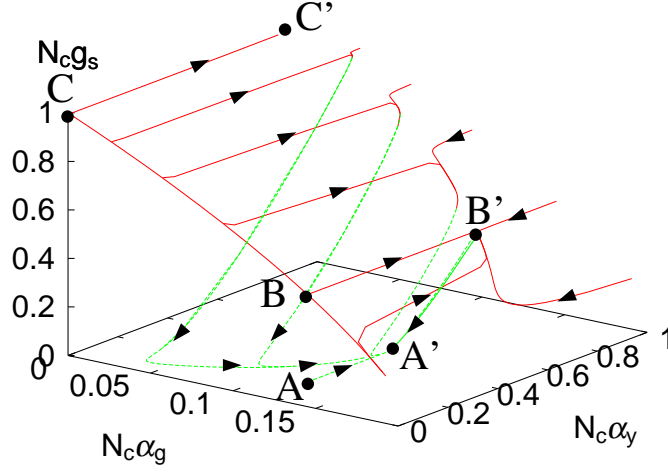


FIG. 9: The RG flows running in the very vicinity of the critical surface are shown in the same case with Fig. 8. The points C and C' represent the UV fixed point of the pure four-fermi theories and of the four-fermi theories with Yukawa interaction.

function given by (8), which depends on the Yukawa coupling at the two-loop level. The beta function for the Yukawa coupling is given by (30), (31) and (32).

As for the four-fermi couplings, let us restrict them to g_S and g_V only for simplicity. Then the beta functions for these couplings are found to be

$$\Lambda \frac{dg_S}{d\Lambda} = (2 + 2\alpha_y)g_S - 2N_c g_S^2 + 2N_f g_S g_V - 12C_2(N_c)\alpha_g g_S + 4\alpha_y g_V \quad (35)$$

$$-18 \frac{C_2(N_c)^2}{N_c} \alpha_g^2 - 6 \frac{C_2(N_c)}{N_c} \left(C_2(N_c) - \frac{N_c}{2} \right) \alpha_g^2, \quad (36)$$

$$\Lambda \frac{dg_V}{d\Lambda} = (2 + 2\alpha_y)g_V + \frac{1}{4}N_f g_S^2 + (N_c + N_f)g_V^2 + \alpha_y g_S - 3 \frac{C_2(N_c)^2}{N_c} \alpha_g^2 - 9 \frac{C_2(N_c)}{N_c} \left(C_2(N_c) - \frac{N_c}{2} \right) \alpha_g^2, \quad (37)$$

where note that the anomalous dimension of the fermion field γ_ψ is not vanishing but is given by the Yukawa coupling in the Landau gauge. In practice, we may find the IR fixed point and the anomalous dimension γ_ϕ^* turns out to be 0.637, when $n_f = 1$. If we take only the ladder diagrams, then the RG equation is reduced to

$$\Lambda \frac{dg_S}{d\Lambda} = (2 + 2\alpha_y)g_S - 2N_c \left(g_S + \frac{3C_2(N_c)}{N_c} \alpha_g \right)^2. \quad (38)$$

Then we may easily evaluate the anomalous dimension at the IR fixed point as $\gamma_\phi^* = 0.65, 0.79, 0.95$ for $n_f = 1, 3, 12$ respectively. Thus fairly large anomalous dimensions may

be realized in the gauge-Yukawa theories with the critical flavor number $N_f = 4N_c$.

VI. RENORMALIZATION OF THE SCALAR POTENTIAL

Renormalization of the scalar potential is peculiar, when the anomalous dimension is large. In this section, we discuss renormalization of the scalar mass m_ϕ^2 and the quartic interaction coupling λ_4 . When we expand the scalar potential at the scale Λ as

$$V(\phi) = \tilde{m}_\phi^2 \Lambda^2 |\phi|^2 + \frac{\lambda_4}{4} |\phi|^4 + \dots, \quad (39)$$

then the RG equations for the dimensionless parameters \tilde{m}_ϕ^2 and λ_4 are found to be

$$\Lambda \frac{d\tilde{m}_\phi^2}{d\Lambda} = -2(1 - \gamma_\phi) \tilde{m}_\phi^2 + 4N_c n_f \alpha_y - 2\tilde{\lambda}_4, \quad (40)$$

$$\Lambda \frac{d\tilde{\lambda}_4}{d\Lambda} = 4\gamma_\phi \tilde{\lambda}_4 - 8N_c n_f \alpha_y^2 + \tilde{\lambda}_4^2, \quad (41)$$

where $\tilde{\lambda}_4 = \lambda_4/(4\pi)^2$ and $\gamma_\phi = 2N_c n_f \alpha_y$.

First we shall discuss analytical solutions of these equations, when the Yukawa coupling stays on the IR fixed point $\alpha_y = \alpha_y^*$. We also take the large N_c leading. Then contributions by the quartic coupling $\tilde{\lambda}_4$ in (40) and (41) may be ignored. Note that the anomalous dimension γ_ϕ^* at the fixed point can be as large as 1 in the strongly coupled case, as was seen in the previous section. Therefore the effective dimension of the scalar mass m_ϕ^2 , which is given by $2(1 - \gamma_\phi^*)$, can be rather small, as N_f approach the critical value. However, m_ϕ^2 is always relevant, since γ_ϕ^* is less than 1.

The solution of the scalar mass at a lower scale μ may be written down as

$$m_\phi^2(\mu) = \left[\tilde{m}_\phi^{*2} + \left(\frac{\Lambda}{\mu} \right)^\epsilon (\tilde{m}_\phi^2(\Lambda) - \tilde{m}_\phi^{*2}) \right] \mu^2, \quad (42)$$

where $\epsilon \equiv 2(1 - \gamma_\phi^*)$ and $\tilde{m}_\phi^{*2} \equiv 2\gamma_\phi^*/\epsilon = \gamma_\phi^*/(1 - \gamma_\phi^*)$. The power of divergence is reduced to ϵ due to the anomalous dimension. As the renormalization scale μ goes down to zero, $m_\phi^2(\mu)$ also decreases to zero irrespectively of the initial value $\tilde{m}_\phi^2(\Lambda)$. Thus the theory on the IR fixed point describes a massless interacting scalar. It should be also noted that \tilde{m}_ϕ^{*2} gives the fixed point value of the dimensionless scalar mass parameter. When \tilde{m}_ϕ^2 is set to this value, the whole theory is scale invariant in the quantum mechanical sense.

Here let us consider the fine-tuning required in order to realize a specific scalar mass $m_\phi^2(\mu) = A\mu^2$ at a low energy scale μ , where A is a parameter of $O(1)$. The degree of

fine-tuning may be given by [24]

$$C = \left| \frac{\delta m_\phi^2(\mu)}{\delta m_\phi^2(\Lambda)} \frac{m_\phi^2(\Lambda)}{m_\phi^2(\mu)} \right|. \quad (43)$$

Then this degree may be evaluated by using the explicit solution (42) and is found to be

$$C = \frac{\tilde{m}_\phi^{*2}}{A} \left(\frac{\Lambda}{\mu} \right)^\epsilon + (A - \tilde{m}_\phi^{*2}). \quad (44)$$

Here the second term may be neglected, since Λ/μ is much larger than 1 when we are concerned about fine-tuning. The degree of fine-tuning C increases, as the cutoff scale Λ is enlarged. Therefore there is maximal value of Λ so that the fine-tuning is remained less than C , and it may be evaluated as $\Lambda = O(1) \times C^{1/\epsilon} \mu$. When $\epsilon = 0.4$, this cutoff scale is 100 times enlarged compared with the case of $\epsilon = 2.0$. Thus fine-tuning problem accompanied by a small scalar mass may be remarkably improved.

On the other hand the anomalous dimension makes the quartic coupling highly irrelevant, since the scaling dimension of λ_4 is given by $4\gamma_\phi^*$ at the IR fixed point. This does not mean that the quartic coupling is eliminated. The RG equation (41) tells us that λ_4 approaches the fixed point value given by

$$\lambda_4^* \simeq |y^*|^2 = \frac{(4\pi)^2}{2N_c n_f} \gamma_\phi^*, \quad (45)$$

very strongly. Similarly the couplings of higher point interactions of the scalar converge to the fixed point values strongly. The presence of the quartic coupling in the RG equation does not alter these renormalization properties.

Lastly we shall consider renormalization of the scalar mass in the theories on the renormalized trajectory from the BZ fixed point. In a general scalar theory, hierarchically small mass cannot be realized, unless the parameter $\tilde{m}_\phi^2(\Lambda)$ given to the cutoff theory is finely tuned to a certain non-zero value. Contrary to this, the CFT of the IR fixed point of the gauge-Yukawa theory may be realized by adding infinitesimally small Yukawa coupling with a *massless free scalar* to the gauge theory on the BZ fixed point.

In Fig. 9, the RG flows in the space of $(\alpha_y, \tilde{m}_\phi^2)$ obtained by solving Eq. (40) are shown in the case of $r = 4.1$ and $n_f = 1$. Then the anomalous dimension at the IR fixed point is found to be $\gamma_\phi^* \simeq 0.65$. The blobs stand for the fixed points $(\alpha_y^*, \tilde{m}_\phi^{2*})$. At the BZ fixed point, the quartic coupling λ_4 is set to zero. The figure shows that there is a renormalized

trajectory connecting these fixed points. The RG flow lines around it show the relatively slow evolution of the mass parameter, which is caused by the large anomalous dimension. Then it is seen that the flows pass vicinity of the IR fixed point can be obtained without fine-tuning of \tilde{m}_ϕ^2 . This behavior is very contrasting compared with the cases with small anomalous dimension. In Fig. 10, the RG flows near the renormalized trajectory towards the IR fixed point are also shown in the case of $r = 5$ and $n_f = 1$ for comparison. In this case the fixed point couplings are rather small and the anomalous dimension is given by $\gamma_\phi^* \simeq 0.08$. It is clearly seen that the RG flows deviate from the renormalized trajectory very easily in sharp contrast with the case of $N_f = 12$. Thus a small scalar mass cannot be realized without tremendous fine-tuning.

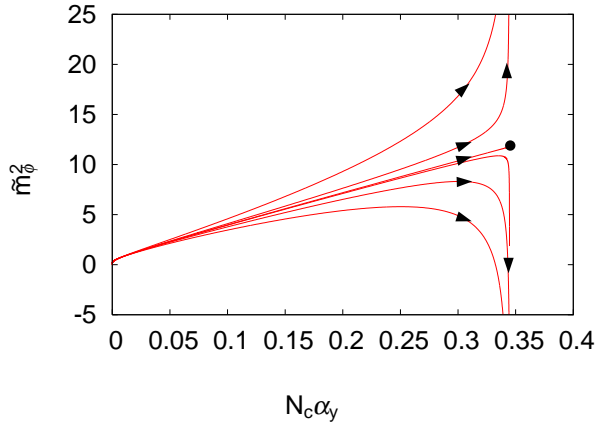


FIG. 10: RG flows of the dimensionless mass parameter \tilde{m}_ϕ^2 in the case of $r = 4.1$ and $n_f = 1$ are shown in the space of $(\alpha_y, \tilde{m}_\phi^2)$. The blobs stand for the fixed points $(\alpha_y^*, \tilde{m}_\phi^{2*})$.

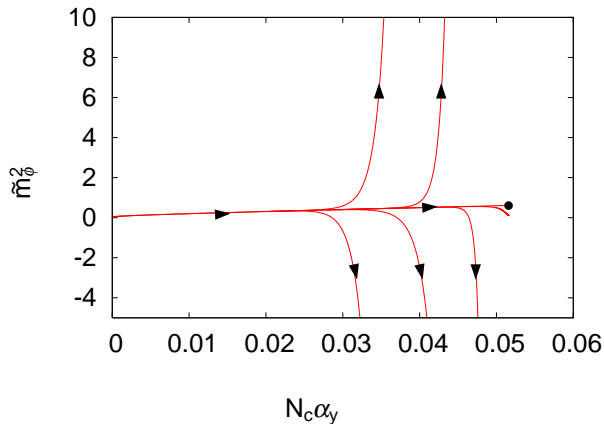


FIG. 11: RG flows of \tilde{m}_ϕ^2 in the case of $r = 5$ and $n_f = 1$ are shown for comparison.

VII. CONCLUSIONS AND DISCUSSIONS

We studied the fixed points and the phase structure of the gauge-Yukawa theories with massless fermions by means of the NPRG. We adopted a somewhat crude approximation scheme, in which the RG equation for the gauge coupling is substituted with the two-loop beta function. However, it was explicitly shown that the approximation beyond the conventional ladder approximation may be applied easily owing to the simplicity of the RG framework. It was also demonstrated through the analysis that the NPRG approach is superior to the DS approach in discussing the fixed points and dynamics around them.

The results of the analysis show that the anomalous dimension of the fermion mass operator can be nearly -1 at the BZ fixed points, when the flavor number is close to the lower edge of the conformal window. Then the Yukawa interaction operator with a scalar field is relevant at the fixed point. We may find that there is the IR fixed point with non-trivial Yukawa coupling in the gauge-Yukawa theories with a flavor singlet scalar. At the IR fixed point, the scalar field acquires a large positive anomalous dimension.

We also discussed the effect of the large anomalous dimension to renormalization of the scalar potential. Especially, the cutoff dependence of the scalar mass squared may be drastically reduced. The other self interactions of the scalar are all irrelevant and the couplings converge to their fixed point values. The scalar mass vanishes as renormalization scale goes to zero due to the anomalous dimension of the fixed point theories. It is found that the gauge-Yukawa theories on the renormalized trajectory give also massless scalars. Thus the gauge-Yukawa theories controlled by the IR fixed point are not annoyed with the fine-tuning problem in order to realize a large mass hierarchy.

In this paper, we have not discussed the dynamics in the broken phase of gauge theories with many flavors, although a lot of studies have been done by the DS approach. We may evaluate the chiral order parameters in the NPRG framework as is shown in Ref. [10]. Especially it is interesting not only theoretically but also phenomenologically to evaluate various order parameters near the critical surface, or near the UV fixed point. For example, the S-parameter and the pion decay constant in the gauge theories with massless flavors slightly less than the critical number have been investigated by solving the Bethe-Salpeter equations as well as the DS equations recently [25]. Such studies seem very interesting in the viewpoint of the phenomenologically viable model building of composite Higgs. Here we

leave these problems to the future works.

Acknowledgements

H.T is supported in part by the Grants-in-Aid for Scientific Research (No. 14540256) and (No. 16028211). from the Ministry of Education, Science, Sports and Culture, Japan.

APPENDIX A: NPRG EQUATIONS FOR THE FOUR-FERMI COUPLINGS

We demonstrate the explicit derivations of the RG equations for the four-fermi couplings given by Eq. (16). The ERG equation is reduced to a set of infinite numbers of one-loop RG equations, once we perform the operator expansion. Evolution of each coupling may be given by reducing the scale of momentum cutoff Λ infinitesimally. This is carried out by integration of the “shell” modes, whose momentum p belongs to $[\Lambda - \delta\Lambda, \Lambda]$, in evaluating the Wick rotated one-loop diagrams. Let us start with the one-loop diagrams inducing the four-fermi couplings, which are illustrated in Fig. 12. We use the Euclidean propagators for the fermion $S(p) = i/\not{p}$ and for the gauge boson

$$D_{\mu\nu}(p) = \frac{1}{p^2} \left(\delta_{\mu\nu} - (1 - \xi) \frac{p_\mu p_\nu}{p^2} \right), \quad (\text{A1})$$

where ξ denotes the gauge parameter.

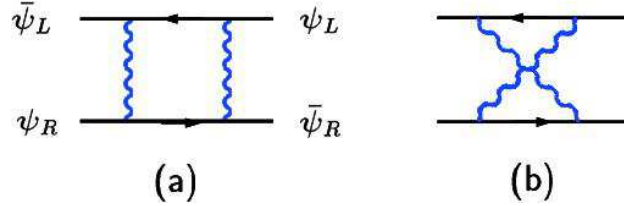


FIG. 12: The four-fermi interaction induced by the gauge interaction at the one-loop level.

The four-fermi operator induced by the box diagram (a) in Fig. 12, which generates the ladder diagrams by solving the NPRG equations, is evaluated as

$$\begin{aligned} \delta\mathcal{L}_{\text{eff}} &= -g^4 \int_{\Lambda - \delta\Lambda < |p| < \Lambda} \frac{d^4p}{(2\pi)^4} D_{\mu\nu}(p) D_{\rho\sigma}(p) \\ &\quad \sum_{AB} \bar{\psi}_{Li} T^A \gamma_\mu S(p) T^B \gamma_\rho \psi_L^i \bar{\psi}_{Rj} T^B \gamma_\sigma S(p) T^A \gamma_\nu \psi_R^j \\ &= \frac{9}{2\Lambda^2} \alpha_g^2 \sum_{AB} \bar{\psi}_{Li} T^A T^B \gamma_\mu \psi_L^i \bar{\psi}_{Rj} T^B T^A \gamma_\nu \psi_R^j \frac{\delta\Lambda}{\Lambda}. \end{aligned} \quad (\text{A2})$$

This operator may be transformed to the operator \mathcal{O}_S given by (12) by using the Fierz identity,

$$\sum_{AB} \bar{\psi}_{Li} T^A T^B \gamma_\mu \psi_L^i \bar{\psi}_{Rj} T^B T^A \gamma_\mu \psi_R^j = -\frac{2}{N_c} C_2(N_c)^2 \bar{\psi}_{Li} \psi_R^j \bar{\psi}_{Rj} \psi_L^i. \quad (\text{A3})$$

Eventually we may obtain a part of the RG equation for the four-fermi coupling g_S as

$$\Lambda \frac{dg_S}{d\Lambda} = 18 \frac{C_2(N_c)^2}{N_c} \alpha_g^2. \quad (\text{A4})$$

In the same way the crossed box diagram (b) in Fig. 12 generates

$$\Lambda \frac{dg_S}{d\Lambda} = 6 \frac{C_2(N_c)}{N_c} \left(C_2(N_c) - \frac{N_c}{2} \right) \alpha_g^2. \quad (\text{A5})$$

This contribution is sub-leading in the large N_c expansion.

It has been found that the summation of these diagrams give a gauge independent corrections for abelian gauge theories [10]. In the non-abelian gauge theories, however, sum of these corrections is gauge depend. In order to make it gauge independent, it would be necessary to incorporate higher dimensional operators such as $\bar{\psi} \sigma_{\mu\nu} \psi F^{\mu\nu}$. We leave this extension for the future study. Rather, in this paper we adopt the Landau gauge.

The other diagrams can be evaluated in a similar manner. Thus the RG equations for the four-fermi couplings given by (16) are found to be

$$\begin{aligned} \mu \frac{dg_S}{d\mu} &= 2g_S - 2N_c g_S^2 + 2N_f g_S g_V + 6g_S g_{V1} + 2g_S g_{V2} \\ &\quad - 12C_2(N_c) \alpha_g g_S - 18 \frac{C_2(N_c)^2}{N_c} \alpha_g^2 - 6 \frac{C_2(N_c)}{N_c} \left(C_2(N_c) - \frac{N_c}{2} \right) \alpha_g^2, \end{aligned} \quad (\text{A6})$$

$$\begin{aligned} \mu \frac{dg_V}{d\mu} &= 2g_V + \frac{1}{4} N_f g_S^2 + (N_c + N_f) g_V^2 - 8g_V g_{V2} \\ &\quad - 3 \frac{C_2(N_c)^2}{N_c} \alpha_g^2 - 9 \frac{C_2(N_c)}{N_c} \left(C_2(N_c) - \frac{N_c}{2} \right) \alpha_g^2, \end{aligned} \quad (\text{A7})$$

$$\begin{aligned} \mu \frac{dg_{V1}}{d\mu} &= 2g_{V1} - \frac{1}{4} g_S^2 - g_S g_V - N_f g_S g_{V2} + 2(N_c - N_f) g_V g_{V1} \\ &\quad + 3g_{V1}^2 + 2(N_c N_f + 1) g_{V1} g_{V2} - \frac{1}{2} \frac{C_2(N_c)}{N_c} \alpha_g g_S, \end{aligned} \quad (\text{A8})$$

$$\begin{aligned} \mu \frac{dg_{V2}}{d\mu} &= 2g_{V2} - 3g_V^2 - (N_f + 2) g_S g_{V1} + (2N_c + 4N_f - 8) g_V g_{V2} \\ &\quad + N_f g_{V1}^2 + (N_c N_f - 2) g_{V2}^2, \end{aligned} \quad (\text{A9})$$

where $g_A = G_A/(4\pi^2)$ ($A = S, V, V1, V2$). The Eqs. (19) and (20) are extracted from the

above equations in the large N_c and N_f leading.

- [1] J.M. Maldacena, *Adv. Theor. Math. Phys.* **2**, 231 (1998); S.S. Gubser, I.R. Kabanov and A.M. Polyakov, *Phys. Lett. B* **428**, 105 (1998); E. Witten, *Adv. Theor. Math. Phys.* **2**, 253 (1998).
- [2] N. Arkani-Hamed, M. Porrati and L. Randall, *JHEP* **0108**, 017 (2001); R. Rattazzi and A. Zaffaroni, *JHEP* **0104**, 021 (2001).
- [3] For a review, see for instance C. Csaki, J. Hubisz and P. Meade, hep-ph/0510275; T. Gherghetta, hep-ph/0601213.
- [4] B.Holdom, *Phys. Lett. B* **150**, 301 (1985); K. Yamawaki, M. Bando and K-I. Matumoto, *Phys. Rev. Lett.* **56**, 1335 (1986); T. Akiba and T. Yanagida, *Phys. Lett. B* **169**, 432 (1986); T.W. Appelquist, D. Karabali and L.C.R. Wijewardhana, *Phys. Rev. Lett.* **57**, 957 (1986); M. Bando, T.Morozumi, H. So and K. Yamawaki, *Phys. Rev. Lett.* **59**, 389 (1987).
- [5] T. Banks and A. Zaks, *Nucl. Phys. B* **196**, 189 (1982).
- [6] For a review see *Dynamical Symmetry Breaking, Proceedings of the 1991 Nagoya Spring School*, edited by K.Yamawaki (World Scientific, Singapore, 1992); V.A. Miransky, *Dynamical Symmetry Breaking in Quantum Field Theories* (World Scientific, Singapore, 1993).
- [7] T. Appelquist, J. Terning and L.C.R. Wijewardhana, *Phys. Rev. Lett.* **77** 1214 (1996); *Phys. Rev. Lett.* **79** 2767 (1997); T. Appelquist, A. Ratnaweera, J. Terning and L.C.R. Wijewardhana, *Phys. Rev. D* **58** 105017 (1998).
- [8] V.A. Miransky and K. Yamawaki, *Phys. Rev. D* **55** 5051 (1997).
- [9] Y. Iwasaki, K. Kanaya, S. Sakai and T. Yoshié, *Phys. Rev. Lett.* **69**, 21 (1992); *Nucl. Phys. B (Proc. Suppl.)* **42**, 502 (1995); Y. Iwasaki, K. Kanaya, S. Kaya, S. Sakai and T. Yoshié, *Nucl. Phys. B (Proc. Suppl.)* **53**, 449 (1997); *Prog. Theor. Phys. Suppl.* **131**, 415 (1998).
- [10] K-I. Aoki, K. Morikawa, J-I. Sumi, H. Terao and M. Tomoyose, *Prog. Theor. Phys.* **97** (1997) 479; *Prog. Theor. Phys.* **102** (1999) 1151; *Phys. Rev. D* **61** (2000) 045008.
- [11] K. Kubota and H.Terao, *Prog. Theor. Phys.* **105**, 809 (2001); H. Terao, *Int. J. Mod. Phys. A* **16**, 1913 (2001).
- [12] H. Gies, J. Jaeckel and C. Wetterich, *Phys. Rev. D* **69**, 105008 (2004); H. Gies and J. Jaeckel, *Eur. Phys. J. C* **46**, 433 (2006).

- [13] M. A. Luty and T. Okui, JHEP **0609** (2006) 070.
- [14] H. Terao, arXiv:0705.0443[hep-ph].
- [15] M.E. Machacek and M.T. Vaughn, Nucl. Phys. B **222**, 83 (1983); Nucl. Phys. B **236**, 221 (1983); Nucl. Phys. B **249**, 70 (1983).
- [16] N. Seiberg, Nucl. Phys. B **435**, 129 (1995); K. Intrilligator and N. Seiberg, Nucl. Phys. Proc. Suppl. **45BC**, 1 (1996).
- [17] A. de Gouvea, A. Friedland and H. Murayama, Phys. Rev. D **59**, 105008 (1999).
- [18] T. Kobayashi and H. Terao, JHEP **0407**, 026 (2004); T. Kobayashi, H. Nakano and H. Terao, Phys. Rev. D **71**, 115009 (2005).
- [19] K. Wilson and J. Kogut, Phys. Rep. **12C**, 75 (1974); F. J. Wegener and A. Houghton, Phys. Rev. A **8**, 401 (1973); J. Polchinski, Nucl. Phys. B **231**, 269 (1984); C. Wetterich, Phys. Lett. B **301**, 90 (1993); M. Bonini, M. D’Attanasio and G. Marchesini, Nucl. Phys. B **409**, 441 (1993).
- [20] S. Arnone, A. Gatti and T.R. Morris, Phys. Rev. D **67**, 085003 (2003); S. Arnone, T.R. Morris and O.J. Rosten, JHEP **0510**, 115 (2005); T.R. Morris and O.J. Rosten, Eur. Phys. J. C **50**, 467 (2007); Phys. Rev. D **73**, 065003 (2006); J. Phys. A **39**, 11657 (2006).
- [21] V.A. Miransky and K. Yamawaki, Mod. Phys. Lett. **A4**, 129 (1989).
- [22] K-I. Kondo, A. Shibata, M. Tanabashi and K. Yamawaki, Prog. Theor. Phys. **91**, 541 (1994).
- [23] T. Brauner and J. Hošek, Phys. Rev. D **72**, 045007 (2005); P. Beneš, T. Brauner and J. Hošek, Phys. Rev. D **75**, 056003 (2007).
- [24] R. Barbieri, and G.F Giudice, Nucl. Phys. B **306**, 63 (1988).
- [25] M. Harada, M. Kurachi and K. Yamawaki, Phys. Rev. D **68**, 076001 (2003); Phys. Rev. D **70**, 033009 (2004); Prog. Theor. Phys. **115**, 765 (2006); M. Kurachi and R. Shrock, JHEP **0612**, 034 (2006); Phys. Rev. D **74**, 056003 (2006).
- [26] The conformal window of $N = 1$ supersymmetric gauge theories is known to be $3/2 < N_f/N_c < 3$ [16]. According to the Seiberg duality, the theories in this window also have a fixed point with a nontrivial Yukawa coupling, when a mesonic chiral superfield is introduced. The RG flows and the fixed points may be explicitly examined [17, 18]. The RG aspect of non-supersymmetric theories is very different from the supersymmetric cases.
- [27] The effective four-fermi operators in QCD with many flavors and their renormalization have been also discussed in Refs. [12]. The RG equations given there may be related with our

results.